Meltdown at Browns Ferry

P.D. Morley[*], Andrew Kalukin[1]

Blue Ridge Scientific LLC Front Royal, VA, 22630, USA

ARTICLE INFO

ABSTRACT

Browns Ferry nuclear power plant (abbreviated BF NPP - three reactors) is located in Northwest Alabama within the New Madrid Seismic Zone (NMSZ) of the North American intraplate fault system. It has the same plan as *Fukushima-Daiichi* NPP in Japan, meaning it has the same design errors which led to the latter's meltdown in 2011 from flooding. Next to BF NPP is the very large Wheeler Reservoir. The NMSZ is capable of generating an 8^+ class moment magnitude earthquake. BF NPP would then be at extreme risk from meltdown due to flooding from Wheeler of the backup diesel generators, both from a turbulent kinetic energy incoherent response, and the far more serious coherent tsunami-seiches response. It is strongly advocated that the Nuclear Regulatory Commission (NRC) create a mitigation plan to safeguard BF NPP, including a possible levee. However, liquefaction flooding with possible Wheeler Reservoir run-in causing inundation, is expected and so the flooding hazard may be an intractable problem. The NRC should include in its mitigation plan facility shutdown. The BF NPP antiquated design is built to only withstand Peak Ground Acceleration (PGA) of 0.1 g (g is the acceleration of gravity). Seismic study of the NMSZ anticipates PGA at BF NPP of around 0.25 g. Thus, ground shocks may disrupt the emergency cooling system from operating, even if the diesels are not flooded.

1. Introduction-what is at stake here

The meltdown[2] at *Fukushima-Daiichi* NPP in Japan would have destroyed Japan had the winds blown North-to-South, instead of West-to-East [1], because it would have then resulted in the evacuation of the Metropolitan Tokyo Region, Fig. 1. While a mega-earthquake from the New Madrid fault (Fig. 2) would destroy the city of Memphis, and cause extensive mid-Atlantic damage [4] (including millions of Americans as internally displaced people), it would be a recoverable catastrophe. In contradistinction, a meltdown at Brown Ferry NPP (Fig. 3) would release enormous amounts of radioactivity in the ground water of mid-America and would not be a recoverable catastrophe. It would make large regions of America uninhabitable and call into question the very future of the United States.

The 2011 Virginia earthquake [5] showed unusual propagation of seismic waves in Eastern United States, due to its granite base. This resulted in shutdown of the North Anna NPP for 2.5 months after design parameters[3] were exceeded [7,8]. The earthquake sequence of events for BF NPP is given in Fig. 4. The control rods will be scrammed as soon as any shock envelope arrives. It is not expected that the three reactor cores will have a problem with scramming, due to the short freefall of the reactor control rods and the fact that most mega-earthquakes have precursor tremors. However, BF NPP is antiquated and has design defects, discussed below. In 2006, the NRC approved 20-year license extensions for all three reactors at BF NPP beyond the original 40-year life of the license [9]. Future life extensions are anticipated. With realistic PGA, both horizontal and vertical, it is expected that some infrastructure damage will occur at BF NPP (with foundations down to bedrock) because its seismic design parameters will be exceeded (like those at North Anna), resulting in a shutdown lasting months or forever (if the turbines are damaged). The purpose of this paper is to show that mega-quake induced flooding by Wheeler Reservoir can lead to meltdown, even if the reactor infrastructure survives.

---

* Corresponding author.
  E-mail addresses: peter3@uchicago.edu (P.D. Morley), kalukin_99@yahoo.com (A. Kalukin).
[1] Guest Researcher.
[2] Disclaimer: the authors are not expressing any political opinion in this article as to whether nuclear energy is 'good' or 'bad'; their only interest is a flooding analysis of a particular NPP in this paper.
[3] This earthquake produced peak ground accelerations (PGA) of 0.27 g at the North Anna NPP [6], which had been designed for core stability PGA of 0.12 g.
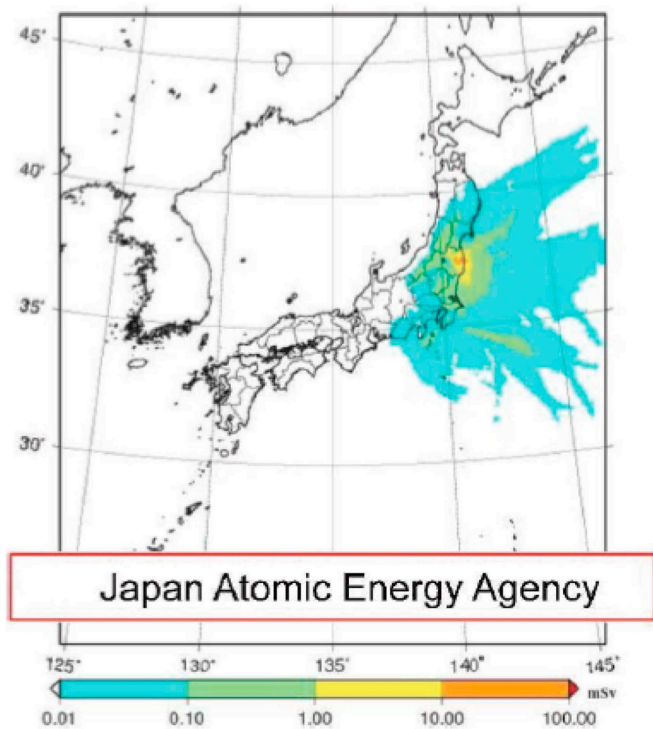
Fig. 1. Nuclear contamination (in units mSv) from the *Fukushima Daiichi* meltdown, taken from Ref. [1].

2. How did the Japanese nuclear engineers get it wrong?

Ordinarily, earthquake flooding is not part of nuclear engineering. It is a part of the civil engineering discipline called geotechnical engineering. However, the Japanese nuclear engineers (considered the elite of the profession) worried about tsunami. *Fukushima Daiichi* reactor complex is the same design as BF NPP. Both have the major design defect of having the critical diesel generators in the basement, below level ground.[4] The Japanese were protected by watertight doors, but the concept of watertight is a static concept. Under cyclic dynamic loading, doors are not watertight. Flooding of the basement diesels will lead to diesel failure and interruption of coolant circulation.

A scientist colleague of the authors obtained the posted tsunami risk technical briefing [11] from the Tokyo Electric Power Company, before it was removed off the Internet. It is quickly seen that the major technical mistake by the Japanese nuclear engineers was the assumption that the earthquake inducing the tsunami was off the coast of South America, where the Nazca oceanic tectonic plate is subducted under the South American continent, Fig. 5. The size of tsunamis is dependent on many factors, and among the most critical, is the distance from the epicenter to the shore. Inexplicitly, the Japanese nuclear engineers did not consult the thousand-year old record of Japan on historical tsunamis. Instead of a Chilean earthquake, the tsunami was generated by an earthquake off the East coast of Honshu, Japan. The protecting sea wall of the *Fukushima Daiichi* NPP was adequate for an accessed 5.2 m tsunami, but the real tsunami height was 14 m. This flooded the diesels as in Fig. 4, interrupting the coolant circulation and causing nuclear core meltdown.[5] The same sequence of events can occur at BF NPP, but instead of Pacific Ocean water, a large inland lake, Wheeler Reservoir,

would be responsible. What does the U.S. Government NRC say?

3. The NRC has deemed BF NPP safe

Though Browns Ferry NPP has been deemed safe by US nuclear regulators, the criteria for assessment of safety have been tied to probabilities of failure derived from laboratory tests of the individual failure of components, and there has been little effort to generate physical models which can account for the **joint probabilities** of multiple extreme disasters occurring at once, in this case earthquake, then flooding. Rigorous statistical analyses have not been completed for American Nuclear Society (ANS) estimates of probability of exceedance of combined flooding events [12,13].

Mitigation against weather-induced flooding is described in the Final Safety Analysis Report for BF NPP; however, tsunami events were explicitly neglected in this report because of the inland setting [14]. Additionally, safety walkdowns and other inspections were performed at BFF NP in response to the Fukushima disaster [15]. These rather comprehensive studies, however, failed to recognize the danger that earthquake-induced flooding poses to NPP, which should be considered a technical mistake.

FEMA/DHS commissioned a study [16] of the expected consequences of a New Madrid seismic rupture. NRC has also studied Browns Ferry using the Seismic Core-Damage Frequency (SCDF) metric, which assesses the safety of Browns Ferry and other US plants based on Individual Plant Examination of External Events. In fact, the nuclear engineering community has done a very good job of recognizing the danger that ground shocks pose for NPP core containment and a very poor job of understanding the risk that flooding presents to NPP that have safely scrammed. The problem is that the NRC has never actually computed a joint probability assessment for rare and high magnitude events. The closest study that the authors were able to find is reference [17].

US nuclear regulators and engineers reconsidered the safety of BF and other NPP in the light of the disaster at Fukushima. The assessment [14] was that an event such as Fukushima was unlikely to occur, because inland events would not lead to the type of tsunami that caused that disaster.[6] The Institute for Energy and Environmental Research (a non-profit [18]) has evaluated [19] the NRC 'Recommendations for Enhancing Reactor Safety in the 21st Century: The Near-Term Task Force Review of Insights from the Fukushima Dai-ichi Accident, U.S. Nuclear Regulatory Commission, July 12, 2011', reference [20], and concluded that the NRC had little understanding of earthquake-induced flooding risks. The NRC conclusion that tsunami-type events cannot occur on in-land lakes will be shown to be a categorically false understanding of physics.

One of the standard tools used by the nuclear industry for assessing flood safety, the flood hazard curve, describes the frequency of exceedance in events per year that a region might experience a flood height greater than a threshold elevation, like a 'hundred year flood'. Climate change has drastically altered the timeline [21]. Earthquake induced flooding contributes to this Probabilistic Risk Assessment (PRA) curve. However, this PRA methodology should be abandoned because of the short historical time window for rare events [22]. What can be done is to model the effects if the extreme event does occur.

BF NPP has several issues that have been documented, calling into question whether the emergency cooling system will even work at all, if the diesels are not flooded. The design of structures and equipment important to the plant safety features was based on a PGA of 0.10 g. In addition, the design is such that the plant can be safely shut down during a PGA of 0.20 g [23]. However, it will be shown in the next

---

[4] This is only one design error. Others include elevated positions of spent fuel pools requiring water to be piped vertically, inability to vent hydrogen through stacks when power is lost, etc. [10].

[5] Even though the nuclear reactor chain reaction has been stopped, decay radioactive heating still continues.

[6] The Japanese nuclear engineers understood the flooding risk and tried to mitigate it. The succeeding sections indicate that the American nuclear engineers do not understand earthquake flooding at all.
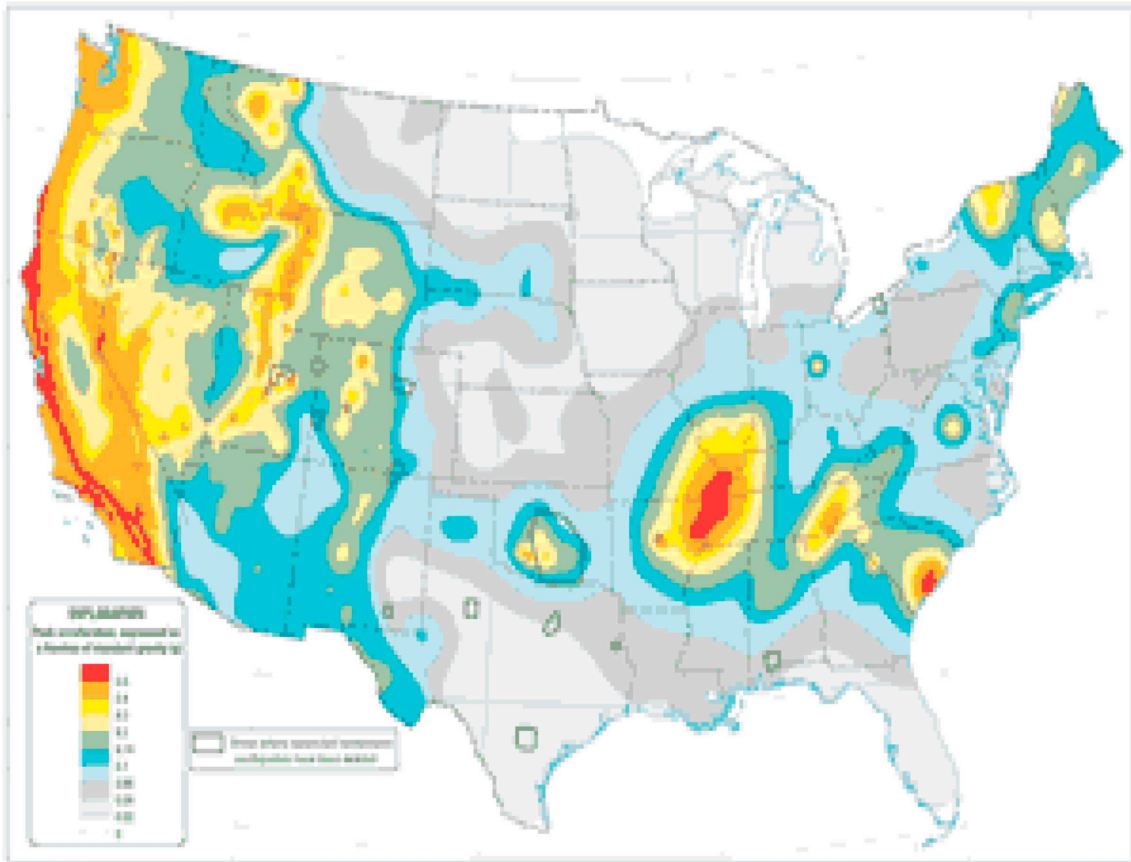
Fig. 2. USGS earthquake hazard zones, showing the New Madrid hazard region. The colors are peak ground accelerations theoretically expected. BF is expected to have PGA ∼ 0.2 g from a moment magnitude 7.7. The symbol g is the acceleration of gravity. From Ref. [2]. (For interpretation of the references to color in this figure legend, the reader is referred to the Web version of this article.)

Fig. 3. Browns Ferry nuclear power plant on the large Wheeler Reservoir (NRC photo from Ref. [3]).

section that expected PGA > 0.25 g. Perhaps, even more worrisome, is the NRC discovery [24] of corruption and mismagement related to the emergency core cooling. For more than two years, BF NPP operated without a fully functioning failsafe system: emergency cooling lines sat blocked and a massive cooling pump did not work.

4. Flooding hazard at BF NPP can be modeled

The authors have undertaken a development of a first-principles seismic-induced flooding model, in lieu of the NRC failure to do so. It should be noted that since the construction of BF NPP, the NMSZ has had thousands of microseismic earthquakes [25]. The physics of
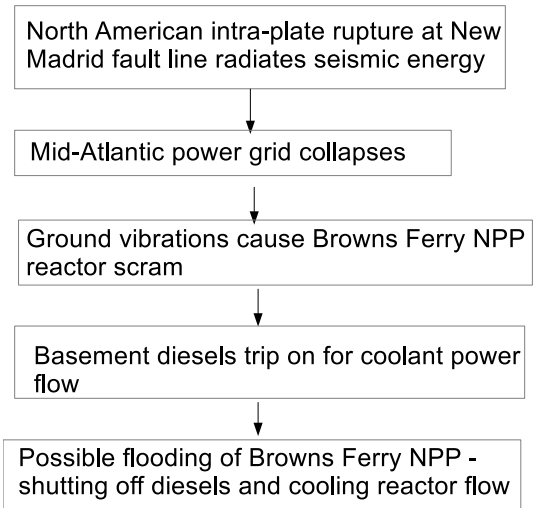

Fig. 4. Sequence of earthquake events leading to meltdown.

earthquake flooding by lakes can be divided into three events:

1. Incoherent lake response: turbulent kinetic energy shoreline flooding
2. Coherent lake response: generation of tsunami/seiche flooding
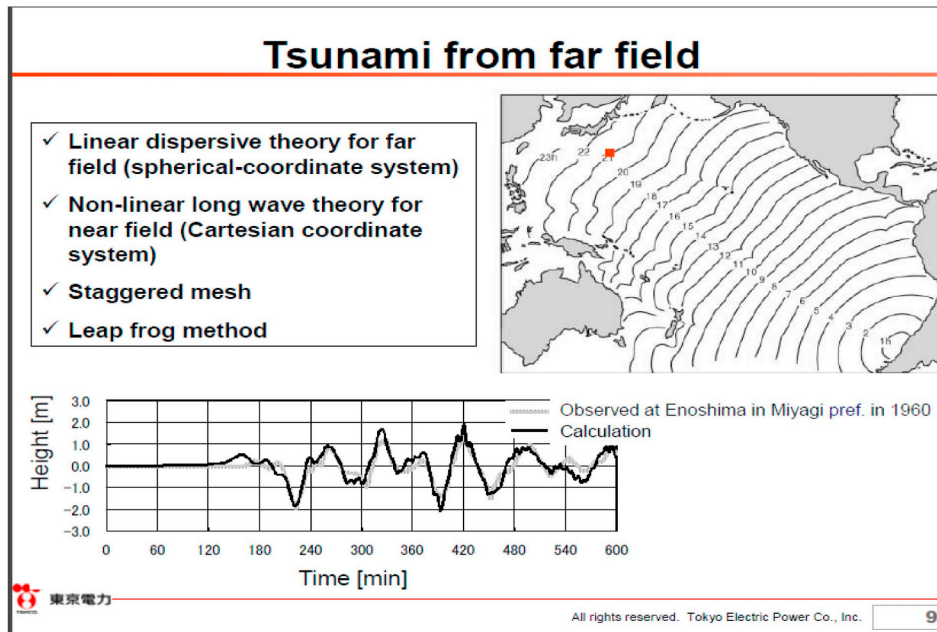3. Liquefaction flooding

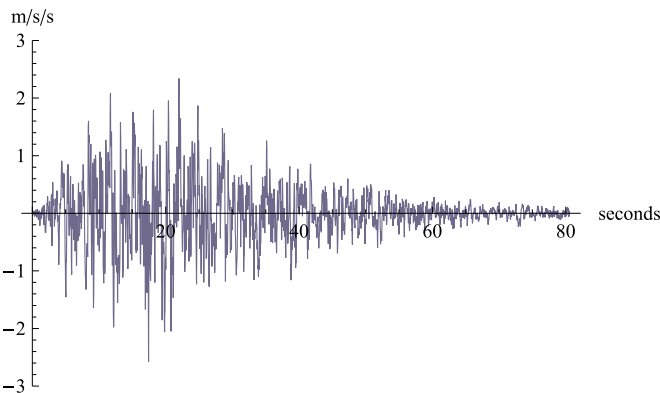**Fig. 5.** Tokyo Electric Power tsunami origin, taken from Ref. [11].
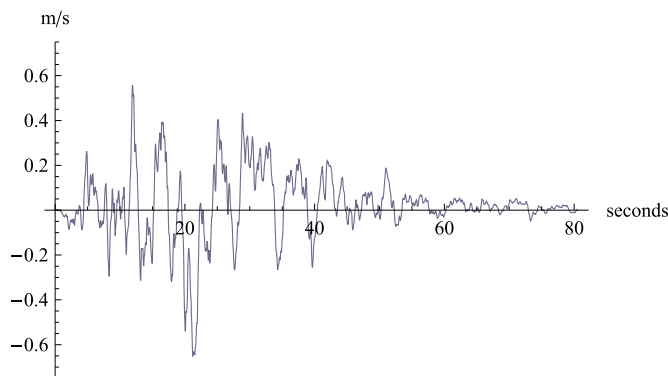
Each of these will be discussed in the following sections.

4.1. Incoherent lake response: shoreline flooding

This is flooding occurring during the earthquake itself.[7] In order to compute an estimate of shoreline flooding from the turbulent kinetic energy of water, synthetic accelerograms must be computed. In appendix A, we consider the size of the possible New Madrid fault earthquake based on geological data. Appendix A shows that an 8^+ class moment magnitude earthquake is possible. In appendix B, we use a moment magnitude 8.0 earthquake to compute synthetic accelerograms based on the stochastic modeling method of references [27,28]. This is the authors' own FORTRAN-95 code.

An example of a synthetic accelerogram, taken from appendix B modeling, is given in Fig. 6. The earth moves in all three directions, so the accelerograms are lateral (X, Y horizontal) and vertical (Z). The PGA are around 0.27 g, in line with Fig. 2. As can be seen, any structure (e.g. limestone cliff) that couples to these seismic waves has a probability of being shaken to collapse.

The response of water to ground motion is different from a free-standing object because water has no cohesive forces maintaining its shape.[8] When the container holding the water undergoes chaotic accelerations, the walls of the container are doing work on the water. An earthquake accelerogram creates chaotic kinetic energy of water turbulence. Even vertical motion creates kinetic energy because the free-surface on top, which would seem not to excite water that has ground motion in the negative vertical direction, results in kinetic energy when the downward ground motion is stopped and the gravitational potential energy drop is converted into kinetic energy. **Thus an earthquake accelerogram is a forcing function of water kinetic energy.** Mathematically, the velocity ground response and the velocity water

Fig. 6. A typical appendix B synthetic accelerogram for ground accelerations.

Fig. 7. Ground velocity profile of Fig. 6.

---

[7] It will be seen in this section that the turbulent kinetic energy of water increases monotonically in time from an earthquake accelerogram. What makes the flooding hazard at BF NPP so dangerous is that during the estimated 80 s earthquake duration, the chaotic kinetic energy becomes so high that a substantial fraction of the basin volume may flood. Since BF NPP is at the lowest part of the shoreline, it will receive a disproportionate fraction of the water.

[8] The reader can do a simple experiment of jiggling a class of water and noting what happens.
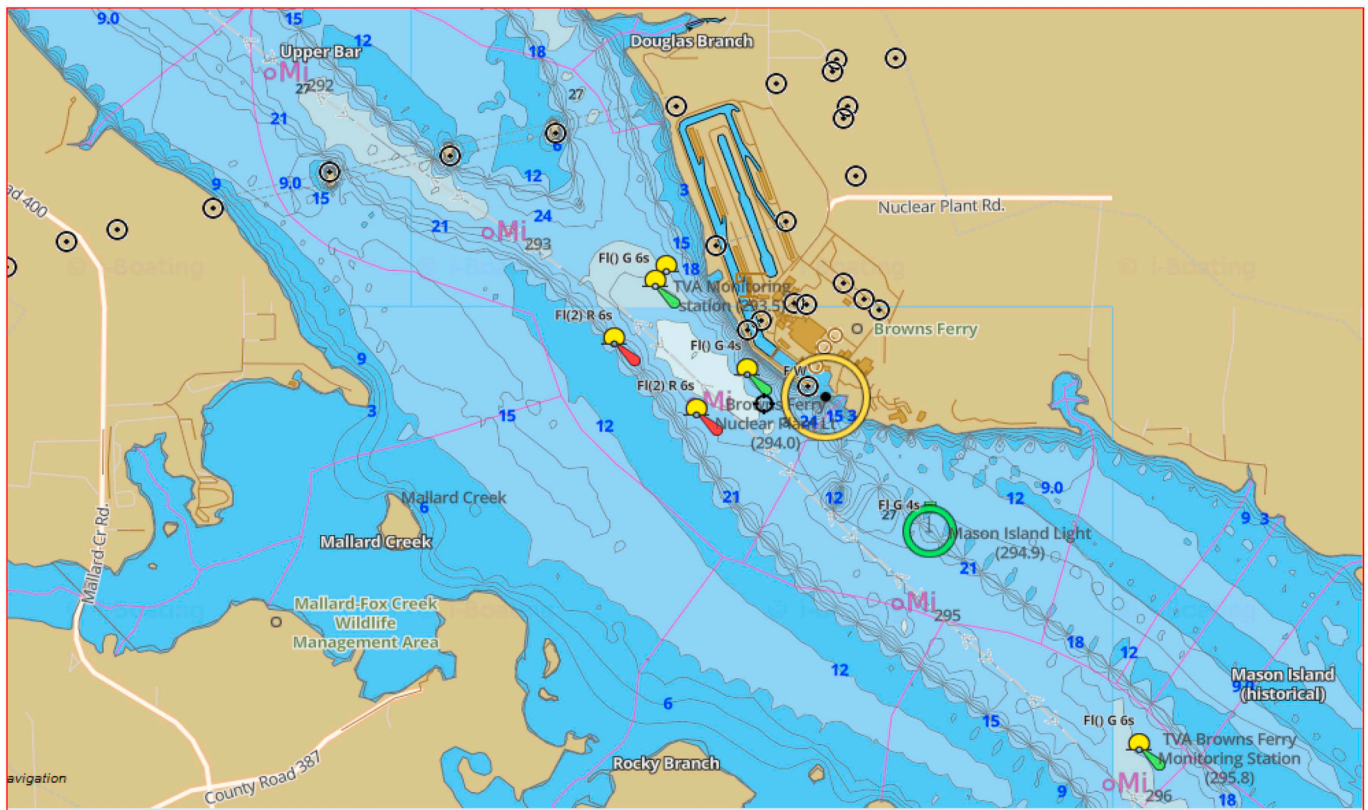
Fig. 8. Bathymetric profile of Wheeler Reservoir reference [26].

Table 1
Estimated shoreline flooding due to 3-dimensional accelerograms.

g·height cut-off	shoreline flooding (acre·feet)	RMS lateral velocity at cut-off (m/s)
2	238.3	2.214
3	658.5	3.131
4	1185	3.835

response to the same accelerogram differ in the following fundamental way:

1. The ground velocity function is a direct integration of the accelerogram, Fig. 7.
2. The water velocity function is a direct integration of the absolute value of the accelerogram.[9]

The different response of water to ground motion means that the longer the duration of the ground motion, the greater is the imparted kinetic energy. For a lake, the turbulent kinetic energy [29] increases to the level that it can overcome the gravitational potential energy of its sidewall, and then afterwards spills over into shoreline flooding. There is a natural cut-off[10] to the turbulent kinetic energy: dissipation energy of the free-surface due to lake wind and wind shear are the primary mechanisms.[11] Indirectly then, the cut-off is proportional to the

gravitational potential energy (per unit mass) of the lip (2 g·*height*, 3 g·*height*, etc.).

The turbulent kinetic energy per unit of mass (KE/M) is $\frac{1}{2}[\overline{V_X^2} + \overline{V_Y^2} + \overline{V_Z^2}]$, where the vector components are the mean-square of the velocity fluctuations, determined by the accelerograms. When this reaches g·*height*, where *height* is the wall height, then spillover begins. After that, statistically 1/3 of the KE/M goes into reaching a greater height after the wall barrier is surmounted, and 1/6 of the KE/M flows horizontially across each vertical face of an imaginary parallelepiped for shoreline flooding, up to the cutoff KE/M.

We assume for Wheeler Reservoir,[12] *height* = 3 m. From Fig. 8, we estimate that BF NPP has a longitudinal exposure of about 2 km. Then Table 1 gives the estimated shoreline flooding[13] as a function of the available cut-offs in the gravitational potential energy of the lip.[14]

The estimated values of shoreline flooding in Table 1 are significant in themselves, independent of coherent response flooding in the sections that follow. What is disconcerting about Table 1 is that the (KE/M) cut-off is not known in advance, but depends on the atmospheric wind/wind shear dissipation interactions with the turbulent free-surface of the lake. It is possible that the actual kinetic energy cut-off occurs later in the accelerogram time history, with consequential vastly increased shoreline flooding.

---

[9] The ensuing positive values are the **root-mean-square** (RMS) velocity fluctuations of each component direction.

[10] An example of water's incoherent response to an accelerogram producing turbulent kinetic energy per mass and having **no** cut-off: water in an in-ground pool. For sufficient forcing time, **all** the water gets sloshed out.

[11] These atmospheric quantities interact with the turbulent kinetic energy of

---

(*footnote continued*)
the water, limiting its maximum value. Internal heat dissipation also occurs. The large earthquake-induced motions are never in equilibrium with dissipation until atmospheric interactions cut in.

[12] The BF NPP has ground elevation of 560 feet [14]. A 3 m *height* means that Wheeler Reservoir has a water elevation of 550.157 feet. In Table 1, the estimated shoreline flooding does not depend on these absolute elevations, but only on the difference.

[13] Averaged over 640 trials, so the expected error is less than one percent.

[14] The assumed 3 m BF NPP lip height is reached after about 12.7 s into the earthquake, for typical accelerograms in 3-dimensions.

Fig. 9. Wheeler Reservoir transverse cross section reference [26].

Fig. 10. Idealized Wheeler Reservoir neck profile.

Fig. 11. The cooling channels that will be resonantly excited by the earthquake wave packet. Photo from Ref. [33].

4.2. Coherent lake response: tsunami-seiches

Seiches are lake oscillations while tsunamis are a special type of water wave, which can reach great heights when breaking onto land. We will treat these separately.

Fig. 12. Wheeler Reservoir is ringed by limestone sedimentary bluffs overlooking the water. Any earthquake induced landsides will create tsunami-like tidal waves that will crash over BF NPP. The most dangerous are actually opposite BF itself, circled. Reference [26].

Fig. 13. Larger scale 3D map showing Wheeler Reservoir ringed by limestone sedimentary bluffs overlooking the water. Some of the high-elevation areas in the vicinity of the reservoir have an elevation of 200 feet above the water. Reference [26].

17.—Slide from Ship Creek delta showing areas of erosion and deposition, and the direction, magnitude, and runup heights of waves. Lines of traverse of wave-damage height are shown in figure 23 and the line of profile A–A' is shown on figure 18.

Fig. 14. Figure taken from Ref. [30] showing slide material and direction of wave travel (arrows). The top numbers on the arrow are runup heights. If similar waves hit the area of BF NPP, they would not be met with a high hillside, so instead of a runup height, they would be associated with massive flooding.

4.2.1. Seiches

Eq (12) gives the period of oscillation of seiches. The neck region, Fig. 9, is the area of Wheeler Reservoir oscillations that will influence BF NPP. With a measured length $L = 1.37$ miles, and a deepest depth 24 feet, with a 12 foot average linear profile, Fig. 10, the longest period is 12.3 min, followed by 369 s, 246 s, 185 s and 148 s for excited multi-mode states. It would seem that these long periods do not couple to the short periods of seismic waves, as expected in the synthetic accel-erograms, which are only a few seconds. This is not true. It is expected that the earthquake shock envelope will cause Wheeler Reservoir to have seiche oscillations many hours after the passage of the seismic waves [30]. Although seiching produces standing waves, these waves become translationary where the water shallows or the lake is con-stricted [30] and seiching creates shoreline flooding. The reason why seismic waves of seemingly different periods excite lake seiches is due to local amplification [31] of long period waves by the water basin.[15] Local amplification of seismic waves has dramatic consequences: the 1985 Michoacan earthquake had epicenter 300 km away from the Mexican City basin, but was amplified [32] by an estimated factor of 10.

BF NPP has cooling channels, Fig. 11, that will themselves undergo seiche oscillation. Using estimated parameters of $L = 30$ m, D = 7 m, the longest period is 7.24 s, while the multi-modes start off at 3.62 s. Thus there is no question that BF NPP will be subjected to seiche flooding over many hours after the cessation of seismic ground vibra-tions. More on seiching in the next section.

4.2.2. Tsunami

The nuclear engineers will be surprised that tsunamis can be gen-erated in inland lakes or bays. During the 1811–1812 New Madrid earthquakes, tsunamis were seen on the Mississippi [34,35]. The me-chanism is landslides (slumps) [36] or land uplift [37]. The uplifted

land can in fact be outside the fault zone [38]. This latter reference does a computational physics model of tsunami/seiches on Lake Tahoe. Waveheight values as high as 10 m are obtained. However, tsunami are deterministic, not stochastic in origin. What can we say about Wheeler Reservoir's exposure to tsunami-type waves? A lot, because Wheeler Reservoir is surrounded by high limestone sedimentary bluffs which overlook the water.[16] Typical examples are in Figs. 12 and 13. Any earthquake-induced landside would result in a tsunami-like wave that will radiate throughout the reservoir. Multiple landsides would create a series of large wave amplitudes that would crash over BF NPP. Slide induced waves and seiching is covered in Ref. [30]. These waves tra-veled onto shore, Fig. 14 with significant waveheights. In Fig. 15, ex-perimental data on earthquake-induced seiches were obtained showing that local amplification of seismic waves can couple long-period seiche oscillations to seismic loading. In Ref. [30], seiching and tsunami-type waves **scoured** the shoreline of Kenai Lake in Alaska.

Finite element modeling may be done to determine structures that are statically stable, but dynamically unstable. The Wheeler Reservoir bluffs, being made of sedimentary limestone, could have landsides from strong ground motion that would be expected to cause significant dis-lodgement.[17]

4.3. Liquefaction flooding

Liquefaction flooding [39] can occur if the water table is close to the surface and if the pressure gradient from the seismic waves is great enough. While the latter constraint is site specific, one can do an em-pirical study relating distance from epicenter to seismic magnitude to get an understanding if the pressure gradient is high enough. This has been done in Ref. [40], where a magnitude 8 quake would be expected

---

[15] This reference [31] gives data showing that the Denali moment magnitude 7.9 earthquake created seiches on inland lakes, from an epicenter 2400 km away.

[16] Readers familiar with the University of Texas @ Austin will recognize that Wheeler Reservoir is very similiar in topography to Lake Travis.

[17] The danger these cliffs pose comes from the fact that the response ampli-tude is greatest at the top of the cliff, and the base itself may act like a lens to amplify seismic waves.

SLIDE-INDUCED WAVES, SEICHING, GROUND FRACTURING AT KENAI LAKE   A27
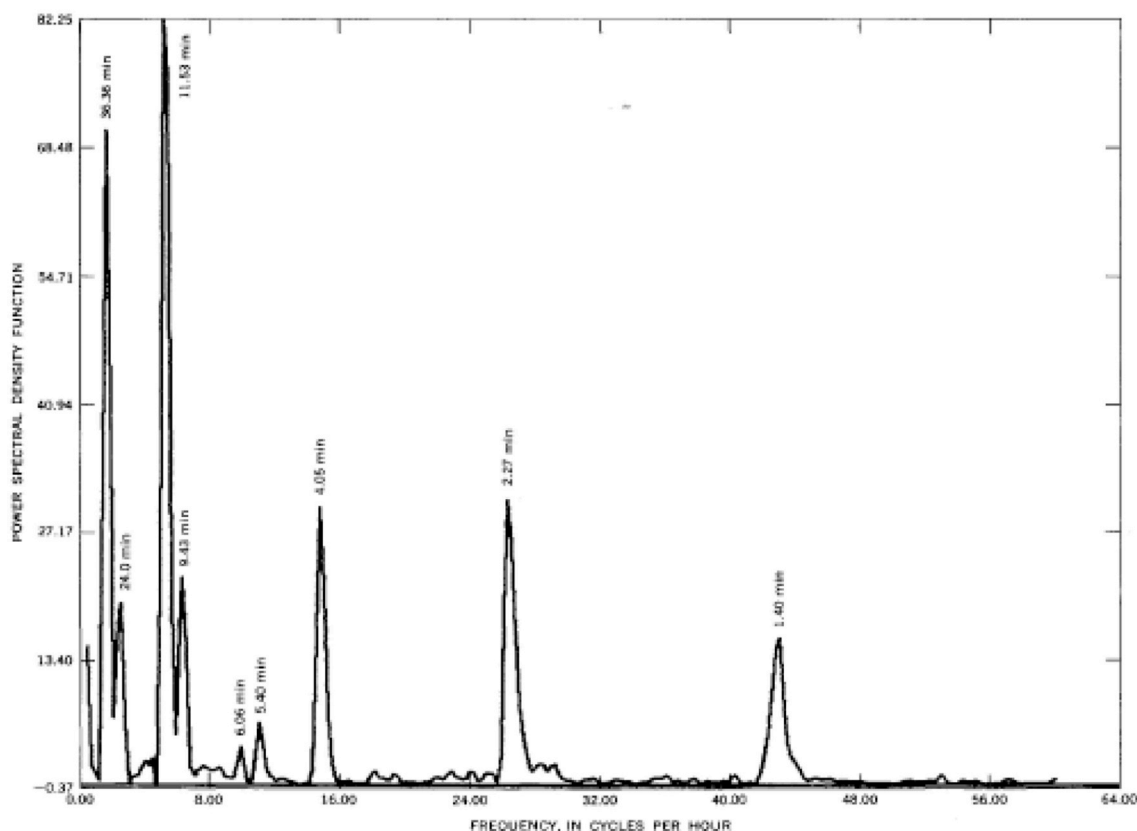
22.—Computed power spectral density function versus the frequency of the seiching recorded on the limnogram at the hydro-electric powerplant. Each peak represents a wave of that frequency, and the periods of these waves (in minutes) are indicated for the larger waves.

Fig. 15. Figure taken from Ref. [30] showing that earthquakes induce lake seiching. The peaks (biggest to smallest) are at: 36.36 min, 24.0 min, 11.53 min, 9.43 min, 6.06 min, 5.40 min, 4.05 min, 2.25 min and 1.40 min. Significantly, the recording equipment was not operational until several hours after the earthquake, showing that seiching carries over many hours after forcing.

to have the potential of liquefaction within a ~ 360 km radius. BF NPP is well within this zone. Since it sits on a large reservoir, the water table may allow this type of flooding. Reference [41] describes liquefaction effects.[18] Buried facilities are very vulnerable to liquefaction flooding. Sand boils erupting water can appear on the protecting side of a levee, compromising its protection. The real damage potential is that the soil separating the cooling channels from BF NPP is breached and total run-in of Wheeler Reservoir occurs. This would lead to full inundation of BF NPP by Wheeler. The NRC already knows that the BF NPP located on the north bank of Wheeler Reservoir at Tennessee River Mile 294.0 has the lowest natural ground elevation in the site vicinity: the Tennessee River above BF NPP site drains 27,130 square miles [14].

5. Conclusion

An intraplate fault earthquake at New Madrid will change America forever. A meltdown at BF NPP is the worst possible outcome - an apocalyptic event[19] for the citizens of the United States. The NRC has

not done a flooding simulation of BF NPP. This paper has done that. Wheeler Reservoir will flood BF NPP: turbulent kinetic energy will cause shoreline flooding during the earthquake itself; seiches will be created lasting many hours and their oscillatory behavior will become flooding when they encounter the BF NPP corner position. Wheeler Reservoir is ringed by limestone sedimentary bluffs which can have landsides, inducing tsunami-type waves that will crash into the nuclear facility. The location of BF NPP immediately adjacent to a large reservoir has high risk of liquefaction flooding.

We strongly advocate that the NRC create a flood mitigation plan, that may include levee protection and should include basin amplification effects folded into finite-element studies. Earthquake resistant

---

[18] This reference gives a very nice example in their Fig. 2, where ground motion is plotted for soils and bedrock. BF NPP sits on bedrock and so the PGA will be maximal.

[19] Most of the meltdown released radioactivity will end up in the Tennessee River and in the ground water of mid-America. We can estimate the lethality of this event as follows: The IAEA [42] estimates that for boiling water reactors,

(footnote continued)

one-GWe generation produces 30 metric tonnes of high-level waste (HLW-requires cooling or special extreme protection). The amount of harmful HLW associated with one tonne is about 2.48×10^6 Ci [43]. Thus 1 GWe creates about 7.46×10^7 Ci. The integrated amount of electrical generation of BF NPP can be estimated to be about 130 GWe, based on the history of the three reactors [44]. The accumulated HLW on-site is then about 9.7×10^9 Ci. We use radioactive Polonium as a surgate for the lethality of HLW, being about 49×10^{-6} Ci [45]. Thus the assessed lethality of a BF NPP meltdown could kill 2×10^{14} human beings. This estimate does not include the much more volumetric low level waste induced-lethality. Radioactive contamination would make mid-America uninhabitable.
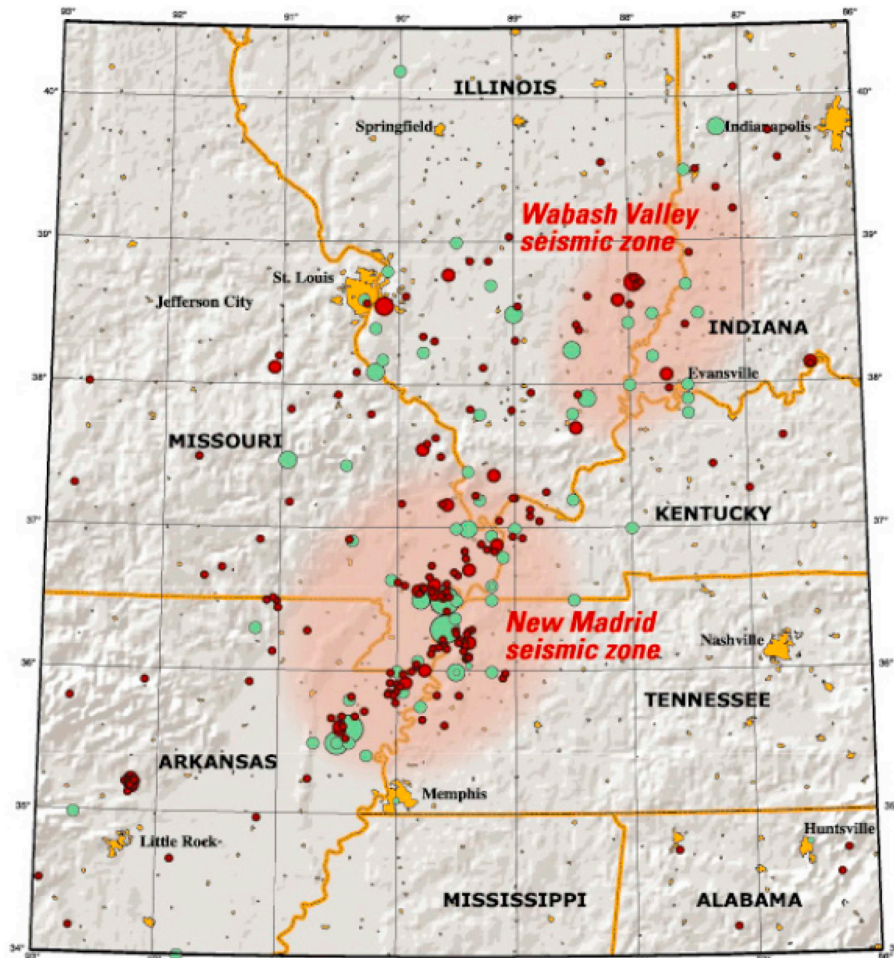
Figure 2. Locations of selected earthquake epicenters larger than M 2.5 in the New Madrid and Wabash Valley Seismic Zones (U.S. Geological Survey, 2002).

Fig. 16. Copy of Qian li et al. [49].

levees are discussed in Ref. [46]. However, liquefaction flooding with possible Wheeler Reservoir run-in causing inundation, is expected and so the flooding hazard may be an intractable problem, given the original site placement. The NRC should include in its mitigation plan facility shutdown.

5.1. New Madrid seismic moment

The Reelfoot Reef, which hosts the New Madrid Seismic Zone, is not a single plane of right lateral strike-slip fracture like the San Andreas fault-line, but a very complicated grouping of ancient convoluted faults. We show in Figs. 16 and 17 the surface contours and locations of recorded earthquakes above Moment 2.5, to give an idea of the geological complexity. In reality, it is numerous faults screwed together, which make multiple mega-earthquakes possible in a short geological time period.

The seismic moment in geo-physics M_S is the torque (units Joule) that two geological formations exert against each other during relative movement. It has the expression [47].

$$M_S = \mu AD \qquad (1)$$

where μ is the shear modulus of the rocks involved, A is the area interface, and D is the relative displacement. For the New Madrid fault system [50], we use idealized quantities: fault-length of 240 km with a vertical depth of 21 km, giving the area $A = 50.4 \times 10^8$ m^2. The rock is granite which has a shear modulus of 27×10^9 Pa [51]. The relation between seismic moment and moment magnitude for great earthquakes

[52] is

$$M = \frac{1}{1.5}[\log M_S - 9.1] \qquad (2)$$

If $M = 8.0$, then $M_S = 1.259 \times 10^{21}$ Joules. This requires a slip $D = 9.25$ m, which is consistent with the slip of great earthquakes [53]. Thus, the New Madrid fault sysystem is capable of 8^+ class moment magnitude North American intraplate earthquakes[20].

5.2. Synthetic accelerograms

In order to estimate the incoherent lake response/turbulent kinetic energy shoreline flooding, we need a good estimate of the ground acceleration, which is a synthetic accelerogram, $A_C(t)$; $A_C(t)$ is a function of time t. This is a convolution of the source function S, with the suitably normalized phase function R

$$A_C(t) = \int_{-\infty}^{+\infty} R(\tau) S(t - \tau) d\tau \qquad (3)$$

The source function has all the physics. The Fourier transform of S will be denoted by notation $A(f)$, where f is frequency.[21] The expected

---

[20] It is of interest to compare the Joules (energy) associated with an 8.0 class moment magnitude earthquake with a large thermonuclear weapon. A megaton thermonuclear weapon has energy 4.184×10^{15} Joules, compared to the 1.259×10^{21} J of a moment magnitude 8.

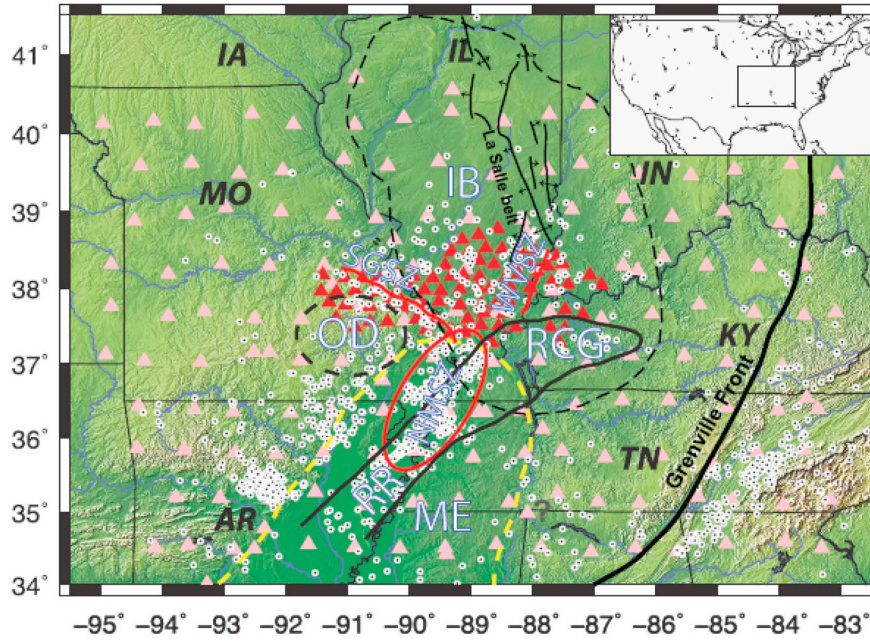[21] We adopt the notation of reference [28].

Figure 1. Location of study area with major geological features. Geological structures are IB, Illinois Basin; OD, Ozark Dome; RR, Reelfoot Rift; RCG, Rough Creek Graben; NMSZ, New Madrid seismic zone; WVSZ, Wabash Valley seismic zone; SGSZ, Ste. Genevieve seismic zone; ME, Mississippi Embayment; La Salle deformation belt; Grenville Front. The intraplate seismic zones are highlighted with red lines. Outlines of major structures were modified from *Buschbach and Kolata* [1991]. Pink triangles denote locations of EarthScope Transportable Array stations and permanent stations, and red triangles denote locations of OIINK (Ozarks-Illinois-Indiana-Kentucky) Flexible Array stations. Black dots are epicenters of M > 2.0 historical earthquakes that occurred between 1 January 1974 and 1 December 2014 from the University of Memphis Center for Earthquake Research and Information (CERI) catalog (http://www.ceri.memphis.edu/seismic/catalogs/cat_nm.html).

Fig. 17. Copy of Chen et al. [48].

duration of the earthquake ground motion is computed as follows: the 240 km fault has a source duration of (240 km/3.5 km/s) where 3.5 km/s is the shear wave velocity of the rock (granite). The radiated seismic waves will have different speeds through the earth because of dispersive effects. This is estimated to have a functional dependence [27] of 10 s per 200 km. BF NPP is 240 km away in this simulation, where from Figs. 16 and 17, this is an average distance.[22] Therefore the total duration of ground shaking expected at BF NPP is around 80.57 s

$A(f)$ is made up of several factors that carry the physics information.

$$A(f) = S_e(f)G(f)A_n(f)P(f)V(f)C_0 M_s [(PRT)R_P(FS)] \tag{4}$$

where.

$S_e(f)$ is the seismological factor

$G(f)$ is the geometric attenuation factor

$A_n(f)$ is the anelastic whole path attenuation factor

$P(f)$ is the upper crust attenuation factor

$V(f)$ is the upper crust amplification factor

C_0 is a scaling factor

M_s is the seismic moment

$[(PRT)R_P(FS)]$ refer to respectively the partition of total shear-wave energy into horizontal components, wave radiation pattern averaged over azimuths, and the free-surface amplification factor.

1. $S_e(f)$ is the 'H96' function from Ref. [27].
2. $G(f) = \frac{1}{70km}\sqrt{130/R}$ where $R = 240$. Taken from Ref. [27].
3. $A_n = exp(p)$, $p = -\pi f \frac{R}{Q\beta}$, $Q = 539 + 152f + 1.43f^2$ reference [28], $\beta = 3.5$ km/s, R in km.
4. $P(f)V(f)$ is given by the function: amdim where amdim = 1.1 for f < 0.1, = 0.0 if f > Nyquist frequency and 1.2087–0.154124*log

(f) $-0.0903987*log(f)*log(f)$ otherwise[23].
5. $C_0 = \frac{1}{4\pi\rho\beta^3}$ where ρ = density of rock at fracture zone (2.75 gm/cm³).
6. $[(PRT)R_P(FS)] = .707 \cdot .55 \cdot 2.$, respectively [27].

For accelerations, a factor $(2\pi i)^2$ multiplies[24] $A(f)$. The normalized phase function is the Gaussian white noise with exponential window, as used in Ref. [27]. The authors' code is in FORTRAN 95.

5.3. Shallow water equations

The shallow water fluid equations play a major role in the flooding assessment of BF NPP by the large Wheeler Reservoir. For one dimensional water oscillation [54] (with horizontal distance parameter x and time t) the equations are

$$\frac{\partial u}{\partial t} = -g\frac{\partial \eta}{\partial x}$$

$$\frac{\partial \eta}{\partial t} = -H\frac{\partial u}{\partial x} \tag{5}$$

If the water does not have a uniform bottom, we can approximate it as an idealized structure (Fig. 10) of deepest depth D, having mean depth $H = D/2$.

The variables are: u one dimensional horizontal velocity vector, averaged across the vertical column and η the total fluid column height. The boundary conditions are

$$u(0) = u(L) = 0 \tag{6}$$

Eq (5) are solved by separation of variables

---

[22] Not the distance to the city of New Madrid, MO.

[23] This is the fitted function $\kappa = 0.08$ in Fig. 12 of reference [27].

[24] The factor $i = \sqrt{-1}$.

$$u(x, t) = T(t)X(x) \tag{7}$$

$$\eta(x, t) = \tau(t)\chi(x) \tag{8}$$

The time dependence is the familiar $T(t) = \tau(t) = e^{-i\omega t}$, giving

$$H\frac{d^2X}{dx^2} + \frac{\omega^2}{g}X = 0 \tag{9}$$

with boundary condition $X(0) = X(L) = 0$. Letting $X(x) = U\sin\alpha x$, Eq (9) reduces to

$$-H\alpha^2 + \frac{\omega^2}{g} = 0 \tag{10}$$

giving

$$\alpha = \frac{\omega}{\sqrt{gH}} \tag{11}$$

The boundary condition $X(L) = 0$ gives $\sin\frac{L\omega}{\sqrt{gH}} = 0$ or $\frac{L\omega}{\sqrt{gH}} = n\pi$. Since the period $\mathscr{P}$ is $\frac{2\pi}{\omega}$, we have finally

$$\mathscr{P} = \frac{2L}{n\sqrt{gH}} \ , \quad n = 1,2, \dots \tag{12}$$

In Eq (12), $n = 1$ is the longest period oscillation, and larger values of n correspond to excited shorter period oscillations.

The physical solutions are (U is a required initial horizontal speed)

$$\eta(x, t) = \mathscr{RE}\left[e^{-i\omega t}\left(\frac{-iHU}{\sqrt{gH}}\right)\cos\frac{\omega x}{\sqrt{gH}}\right] \tag{13}$$

$$u(x, t) = \mathscr{RE}\left[e^{-i\omega t}U\sin\frac{\omega x}{\sqrt{gH}}\right] \tag{14}$$

where $\mathscr{RE}$ means real value. This seiche solution gives the periodicity of the waves.

References

[1] Takeo Ohnishi, The disaster at japans fukushima-daiichi nuclear power plant after the march 11, 2011 earthquake and tsunami, and the resulting spread of radio-isotope contamination, Radiat. Res.: January 177 (No. 1) (2012) 1–14.

[2] https://earthquake.usgs.gov/hazards/hazmaps/.

[3] https://en.wikipedia.org/wiki/Browns_Ferry_Nuclear_Plant.

[4] http://cusec.org/.

[5] 2011 Virginia Earthquake, https://en.wikipedia.org/wiki/2011_Virginia_earthquake.

[6] https://www.iitk.ac.in/nicee/wcee/article/WCEE2012_3494.pdf.

[7] citeseerx.ist.psu.edu/viewdoc/download?doi=10.1.1.817.9895&rep=rep1&type=pdf.

[8] The 2011 Virginia Earthquake: what Are Scientists Learning, https://agupubs.onlinelibrary.Wiley.com/doi/epdf/10.1029/2012EO330001.

[9] TVA Boosting Power Output at Browns Ferry with $475 Million Upgrade, https://www.timesfreepress.com/news/breakingnews/story/2018/feb/20/tva-boosts-power-output/464144/.

[10] J. Buongiorno et al, 'Technical Lessons Learned from the Fukushima Daiichi Accident and Possible Corrective Actions for the Nuclear Industry: an Initial Evaluation', Center for Advanced Nuclear Energy Systems, MIT, ML11347A455_fukushima_lessons_learned_NRC.pdf.

[11] 'Tsunami Technical Assessment for Nuclear Power Plants in Japan', Makato Takao, Tokyo Electric Power Company.

[12] Rajiv Prasad, Lyle F. Hibler, Andre M. Coleman, Duane L. Ward, Design Basis Flood Estimation for Site Characterization at Nuclear Power Plants in the United States of America, NUREG/CR-7046 US NRC, 2011 available at https://www.nrc.gov/docs/ML1132/ML11321A195.pdf.

[13] Nuclear Energy Institute, External Flooding Assessment Guidelines, NEI 16-05, April 2016; available at https://www.nrc.gov/docs/ML1615/ML16159A077.pdf.

[14] Flood Hazard Evaluation Report for Browns Ferry Nuclear Plant, https://www.nrc.gov/docs/ML1507/ML15072A130.pdf.

[15] Follow-up to the Fukushima Daiichi Nuclear Station Fuel Damage Event, (May 13, 2011) https://www.nrc.gov/docs/ML1113/ML111330509.pdf.

[16] http://hdl.handle.net/2142/14810.

[17] G. Martinez-Guridi, J. Lehner, Scoping Study for a PRA Method for Seismically Induced Fires and Floods, Final Report, December, 2015 NRC JCN vol 6400.

[18] http://www.ieer.org.

[19] IEER-review-of-NRC-Fukushima-Task-Force-Review2011-07-12.pdf, available at

[20] http://www.ieer.org.

[20] Charles Miller, et al., Recommendations for enhancing reactor safety in the 21st Century, available https://www.nrc.gov/docs/ML1118/ML111861807.pdf.

[21] Chris Flavelle, C. Jeremy, F. Lin, U.S. Nuclear Plants Weren't Built for Climate Change, (2019) Bloomberg Buisnessweek April 18 https://www.bloomberg.com/graphics/2019-nuclear-power-plants-climate-change/.

[22] Ray Schneider, Perspectives on External Flooding Probabilistic Risk Assessment: Gaps and Challenges Risk Analyst Perspective, (2017) NRC 3rd annual flood workshop https://adamswebsearch2.nrc.gov/webSearch2/main.jsp?AccessionNumber=ML17355A077.

[23] Tennessee Valley Authority's Seismic Hazard and Screening Report, https://www.nrc.gov/docs/ML1409/ML14098A478.pdf.

[24] Challen Stephens, Browns Ferry: Shrinking the Safety Margin at Alabama's Largest Nuclear Plant, http://blog.al.com/wire/2013/07/browns_ferry.html.

[25] Facts about the New Madrid Seismic Zone, https://dnr.mo.gov/geology/geosrv/geores/techbulletin1.htm.

[26] www.usgs.gov.

[27] M. David, Boore, 'Simulation of ground motion using the stochastic method', Pure Appl. Geophys. 160 (2003) 635–676.

[28] Nelson Lam, John Wilson, Graham Hutchinson, Generation of synthetic earthquake accelerograms using seismological modeling: a review, J. Earthq. Eng. 30 (Apr) (2008) 321–354.

[29] https://en.wikipedia.org/wiki/Turbulence_kinetic_energy.

[30] D. S. McCulloch, 'Slide-induced Waves, Seiching and Ground Fracturing Caused by the Earthquke of March 27, 1964 at Kenai Lake, Alaska', US Geological Survey Professional Paper 543-A, available at https://pubs.usgs.gov/pp/0543a/.

[31] Aggeliki Barberopoulou, et al., Local amplification of seismic waves from the Denali earthquake and damaging seiches in lake union, seattle, Washington, Geophys. Res. Lett. 31 (2004) L03607, https://doi.org/10.1029/2003GL018569.

[32] Francisco J. Chavez-Garcia, Pierre-Yves Bard, Site effects in Mexico City eight years after the September 1985 Michoacan earthquakes, Soil Dynam. Earthq. Eng. 13 (1994) 229–247.

[33] archive.knoxnews.com/business/tva-reports-detail-issues-at-browns-ferry-after-april-tornadoes-ep-403693805-357673621.html/?page=1.

[34] P.A. Lockridge, L.S. Whiteside, J.F. Lander, Tsuanmis and tsunami-like waves of the Eastern United States, Sci. Tsunami Hazards 20 (3) (2002) 120–157.

[35] Rajiv Prasad, Tsunami Hazard Assessment at Nuclear Power Plants in the United states of America', NUREG/CR-6966, (March 2009) available at https://www.nrc.gov/docs/ML0915/ML091590193.pdf.

[36] Michael Schnellmann, et al., Prehistoric earthquake history revealed by Lacustrine slump deposits, Geology (2002) 30 1131 available at https://pubs.geoscienceworld.org/gsa/geology/article-abstract/30/12/1131/192305/prehistoric-earthquake-history-revealed-by-Lacustrine-slump-deposits.

[37] Wm G. Van Dorn, 'Source Mechanism of the Tsunami OP MARCH 28, 1964 in Alaska", Scripps Institution of Oceanography, La Jolla, California, 2304-10135-1-PB.pdf.

[38] Gene A. Ichinose, et al., The potential hazard from tsunami and seiche waves generated by large earthquakes within Lake Tahoe, California-Nevada, Geophys. Res. Lett. 27 (8) (2000) 1203–1206. APRIL 15.

[39] https://pnsn.org/outreach/earthquakehazards/.

[40] Gerassimos A. Papadopoulos, Georgios Lefkopoulos, Magnitude-distance relations for liquefaction in soil from earthquakes, Bull. Seismol. Soc. Am. 83 (1998) 925.

[41] Misko Cubrinovski, et al., Geotechnical aspects of the 22 february 2011 christchurch earthquake, Bull. N. Z. Soc. Earthq. Eng. 44 (No. 4) (December 2011) 205–226.

[42] IAEA-TECDOC-1591, Estimation of Global Inventories of Radioactive Waste and Other Radioactive Materials, (2008) available at https://www-pub.iaea.org/MTCD/Publications/PDF/te_1591_web.pdf.

[43] https://www.radioactivity.eu.com/site/pages/HLW_Waste.htm.

[44] https://www.tva.gov/Energy/Our-Power-System/Nuclear/Browns-Ferry-Nuclear-Plant.

[45] https://en.wikipedia.org/wiki/Polonium.

[46] Yasushi Sasaki, et al., Reconnaissance report on damage in and around river levees caused by the 2011 off the pacific coast of tohoku earthquake, Soils Found. 52 (5) (2012) 1016–1032.

[47] https://en.wikipedia.org/wiki/Seismic_moment.

[48] C. Chen, H. Gilbert, C. Andronicos, M.W. Hamburger, T. Larson, S. Marshak, G.L. Pavlis, X. Yang, Shear velocity structure beneath the central United States: implications for the origin of the Illinois Basin and intraplate seismicity, Geochem. Geophys. Geosyst. 17 (2016) 1020–1041, https://doi.org/10.1002/2015GC006206.

[49] Li Qian, E.W. Woolery, M.W. Crawford amd, D.M. Vance, Seismic velocity database for the New Madrid seismic zone and its vicinity, Kentucky Geol. Surv. Inf. Circ. 27 (2013) Series XII.

[50] https://en.wikipedia.org/wiki/New_Madrid_Seismic_Zone.

[51] https://en.wikipedia.org/wiki/material-properties/Granite.

[52] L. Liberatore, L. Sorrentino, D. Liberatore, 'Engineering Analysis of Ground Motion Records of Chile, 2010 Earthquake', 15th World Conference on Earthquake Engineering, Lisbon, Portugal, (2012) available at https://www.iitk.ac.in/nicee/wcee/article/WCEE2012_5381.pdf.

[53] Marcelo Farias, et al., Land-Level Changes Produced by the M_w 8.8 2010 Chilean Earthquake, available at https://www.science.sciencemag.org/content/329/5994/916.

[54] Shallow Water Equations, https://en.wikipedia.org/wiki/Shallow_water_equations.